

Special
Collection

Synthesis and Structure–Activity Relationships of Imidazopyridine/Pyrimidine- and Furopyridine-Based Anti-infective Agents against Trypanosomiasis

Daniel G. Silva,^{*,[a, b]} Anna Junker,^[b] Shaiani M. G. de Melo,^[a] Fernando Fumagalli,^[c] J. Robert Gillespie,^[d] Nora Molasky,^[d] Frederick S. Buckner,^[d] An Matheeußen,^[e] Guy Caljon,^[e] Louis Maes,^[e] and Flavio S. Emery^{*,[a]}

Neglected tropical diseases remain among the most critical public health concerns in Africa and South America. The drug treatments for these diseases are limited, which invariably leads to fatal cases. Hence, there is an urgent need for new antitrypanosomal drugs. To address this issue, a large number of diverse heterocyclic compounds were prepared. Straightforward synthetic approaches tolerated pre-functionalized structures, giving rise to a structurally diverse set of analogs. We report on a set of 57 heterocyclic compounds with selective

activity potential against kinetoplastid parasites. In general, 29 and 19 compounds of the total set could be defined as active against *Trypanosoma cruzi* and *T. brucei brucei*, respectively (antitrypanosomal activities < 10 μ M). The present work discusses the structure–activity relationships of new fused-ring scaffolds based on imidazopyridine/pyrimidine and furopyridine cores. This library of compounds shows significant potential for anti-trypanosomiasis drug discovery.

Introduction

Trypanosomiasis caused by the unicellular protozoan parasites *Trypanosoma brucei* and *T. cruzi* are economically significant obstacles to human welfare. Human African Trypanosomiasis

(HAT) caused by *T. brucei* occurs in Sub-Saharan Africa, while Chagas disease caused by *T. cruzi* is a devastating disease in Latin America.^[1] The current drug treatments available for these diseases are toxic, prone to resistance, and poor/limited efficacy.^[2–7] Developing a new drug is a laborious challenge, and investments dedicated to the identification of new chemical entities (NCEs) for the treatment of infectious diseases are insufficient.^[8,9] Existing infrastructures to prevent and combat Chagas disease and HAT are largely inadequate and therefore, these have been classified as Neglected Tropical Diseases (NTDs).

A previous phenotypic high-throughput screening of a 700,000 compounds library performed by the Genomics Institute of the Novartis Research Foundation (GNF) led to the identification of 1035 compounds that inhibited in vitro growth of *T. brucei* at concentrations below 3.6 μ M and were non-toxic to mammalian cells (Huh7). The lead compound **A** (thiazol-2-ethylamine derivative) was one of the scaffolds selected for optimization by researchers at the University of Washington and North Carolina at Chapel Hill (UNC).^[10] The most potent and selective compound **A** against *T. brucei* showed poor metabolic stability (Figure 1) as demonstrated by its short half-life in mice and human liver microsomes.^[11] To overcome the metabolic stability issues, Patrick and coworkers^[12] synthesized a new series of compounds based on urea derivatives of 2-aryl-benzothiazol-5-amines.

The most promising benzothiazole compound **B** was a new lead against *T. brucei* (EC₅₀ of 0.03 μ M; Figure 1).^[12] Guided by these previous studies Silva and coworkers^[13] further modified the benzothiazole core of **B** to the imidazopyrimidine rings in compounds **C** and **D**. A basic nitrogen atom inserted at the 6-position of the imidazopyrimidine core resulted in the most significant increase in activity with a 1000-fold change in EC₅₀

[a] Dr. D. G. Silva, S. M. G. de Melo, F. S. Emery
QHeteM - Laboratório de Química Heterocíclica e Medicinal
School of Pharmaceutical Sciences of Ribeirão Preto – University of São Paulo
Ribeirão Preto, São Paulo 14040-903 (Brazil)
E-mail: danielgedder@usp.br
flavioemery@usp.br

[b] Dr. D. G. Silva, Dr. A. Junker
European Institute for Molecular Imaging (EIMI)
Westphalian Wilhelms-University
48149 Münster (Germany)

[c] Prof. F. Fumagalli
Centro de Ciências da Saúde (CCS)
Universidade Federal de Santa Maria (UFSM)
Av. Roraima, 1000
Camobi, Santa Maria, Rio Grande do Sul, 97105-900 (Brazil)

[d] J. R. Gillespie, N. Molasky, Prof. F. S. Buckner
Department of Medicine
University of Washington
Seattle, WA 98195 (USA)

[e] A. Matheeußen, Prof. G. Caljon, Prof. L. Maes
Laboratory of Microbiology, Parasitology and Hygiene (LMPH)
University of Antwerp
Universiteitsplein 1
Antwerpen, 2610 Wilrijk (Belgium)



Supporting information for this article is available on the WWW under <https://doi.org/10.1002/cmdc.202000616>



This article belongs to the Special Collection "BrazMedChem 2019: Medicinal Chemistry in Latin America".



© 2020 The Authors. ChemMedChem published by Wiley-VCH GmbH. This is an open access article under the terms of the Creative Commons Attribution Non-Commercial License, which permits use, distribution and reproduction in any medium, provided the original work is properly cited and is not used for commercial purposes.

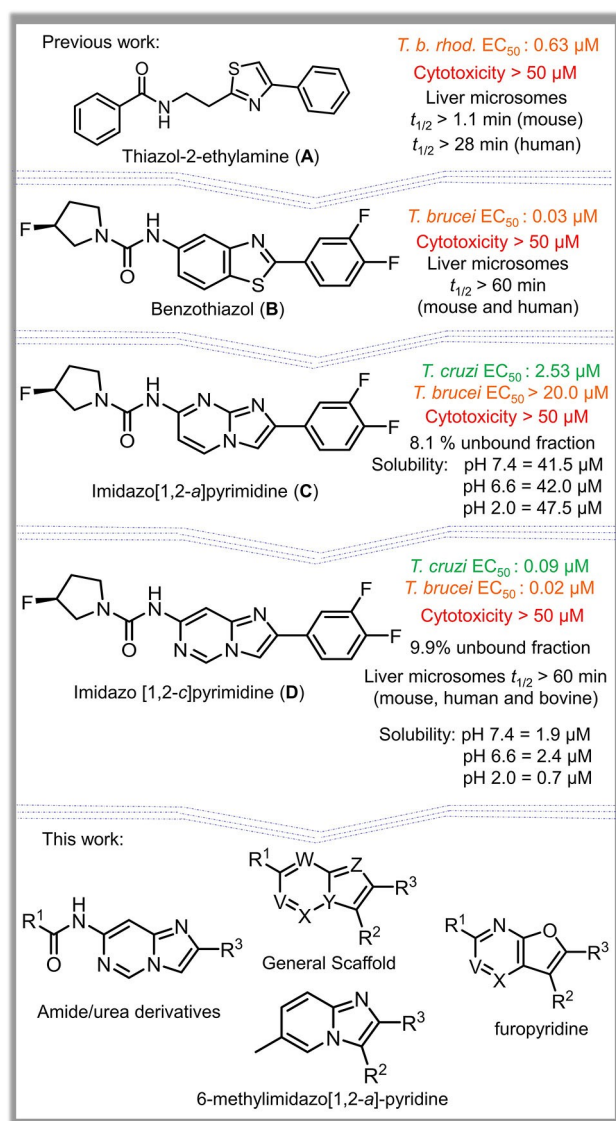


Figure 1. TOP: initial compound designed for the treatment of HAT (A). BELOW: benzothiazole B and imidazopyrimidines C and D compounds. Antitrypanosomal activities highlighted in green and orange. BOTTOM: set of compounds planned, synthesized, and assayed against *T. cruzi*, *T. brucei* and mammalian cells in the present work.

against *T. brucei* (C vs D). The main results of our previous works^[11–14] are summarized in Figure 1.

Based on promising in vitro activity, cytotoxicity, metabolic stability, protein binding and pharmacokinetic (PK) properties, the imidazo[1,2-c]pyrimidine derivative D was selected as a candidate for in vivo follow-up studies in an acute mouse model of *T. cruzi* infection (Tulahuen strain). After established infection, mice were dosed twice daily for 5 days and monitored for 6 weeks using an in vivo imaging system (IVIS)^[13] demonstrating parasite inhibition comparable to benznidazole. Scaffold D had alterations primarily at either of the two terminal rings, but the SAR of the internal portion of the molecule remained largely unexplored.^[13]

Drug discovery and development is a complex endeavor since new candidates need to meet acceptable pharmacological endpoints combined with favorable safety profiles. Moving from target identification to lead generation is laborious, but our compound D may represent a potential hit for trypanosomiasis^[13] and was therefore studied further in the present work.

Imidazopyridine/pyrimidine fused rings have been employed in drugs such as antipsychotics, anxiolytics, analgesics, and migraine therapeutics, demonstrating drug-like features associated with the core structures.^[10,15–17] The furo[2,3-b]pyridine has recently received extensive attention as a useful pharmacophore in different therapeutic areas.^[18–21] We also identified promising selective bioactive compounds containing furo[2,3-b]pyridine as a central core against different drug-resistant strains of mycobacteria for tuberculosis.^[22] However, this class of compound has not yet been employed for antitrypanosomal agents.

To enlarge the chemical space of heterocycles as potential anti-infective agents against trypanosomiasis, we aimed to explore, develop, and modify the central core of the hit compound D (bottom of Figure 1) and perform SAR analysis based on biological assays against *T. cruzi*, *T. brucei*, and mammalian cells.

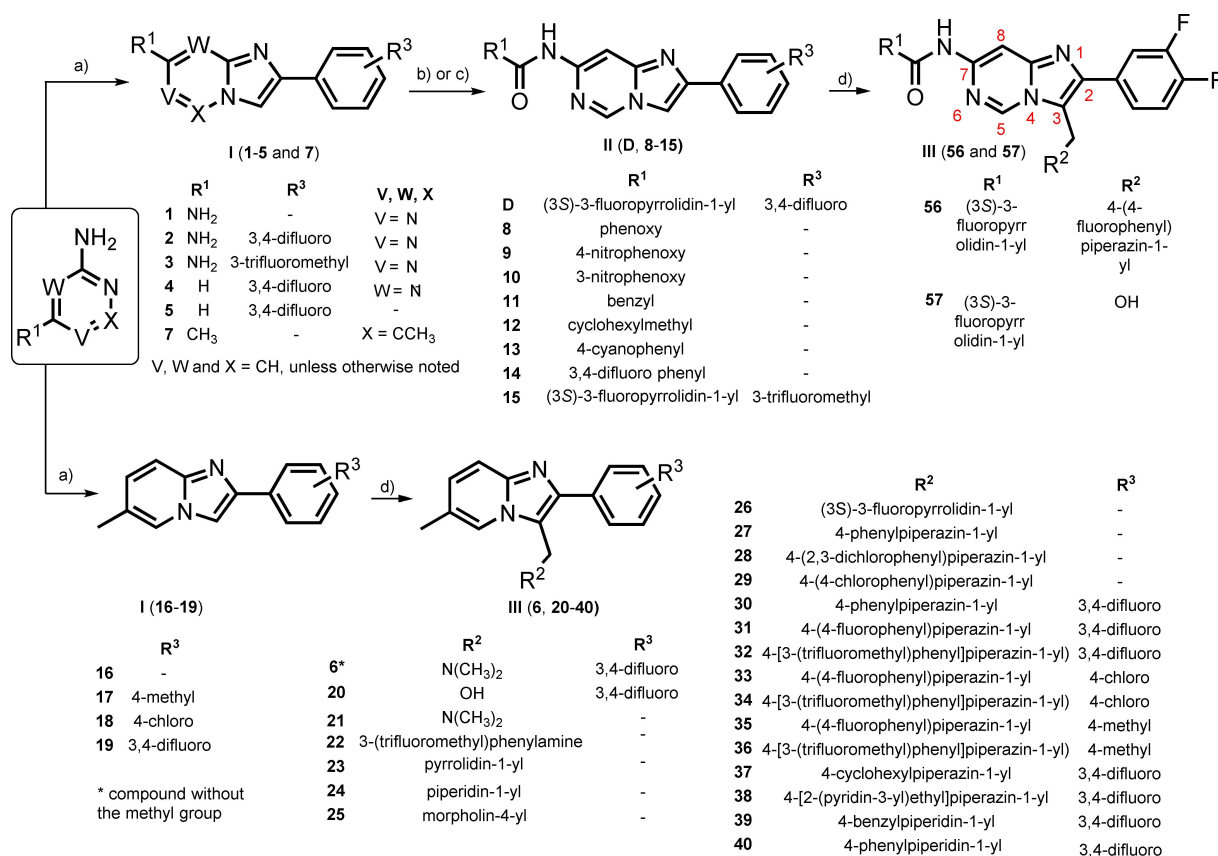
Results and Discussion

Designed library and synthesis of heterocycles

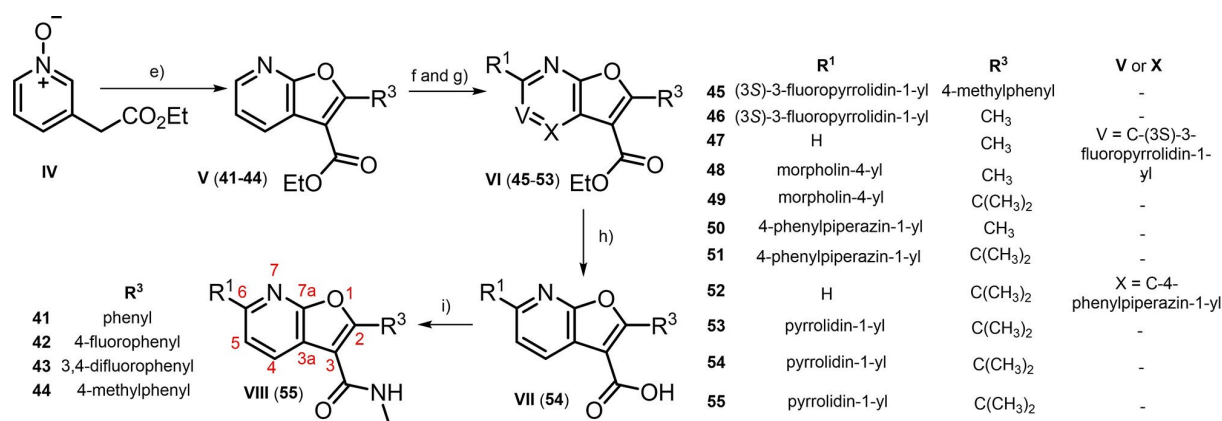
The biochemical targets or mechanisms of action of the hit compound D are unknown. A new set of compounds was designed by dividing the general scaffold (Figure 1) into regions and specific insertion of modifications at the positions V–Z and in regions R¹–R³ on the central core of the fused ring. The modifications to the general scaffold are shown in Schemes 1 and 2.

A relatively simple synthetic pathway (low cost, few steps and good yields) was amenable to many functional groups, giving rise to a structurally diverse set of analogs (Scheme 1). Synthesis of the compounds 1–5, 7 and 16–19 started with a condensation reaction of the appropriate amino pyrimidine/pyridine and bromoacetophenone, which resulted in the intermediate endowed with the imidazopyrimidine or imidazopyridine cores (I). Following the reaction with triphosgene, a corresponding isocyanate was obtained, which provided a way for the formation of urea derivatives D and 15 (II). The reaction with the appropriate acyl chloride provided the amide derivatives 8–14 (II). Upon Mannich reaction, we explored amino-alkylations in region R² of the imidazopyrimidine/pyridine scaffold III (analogs 6, 20–40, 56 and 57).

Compounds 1–3 are imidazopyrimidine fragment-like containing a free amine group (R¹) and bearing different phenyl groups at the 2-position of the imidazole portion of the backbone. Compound 4 is an analog of compound 2 without the free amine and the pyrimidine nitrogen at the position W. Compounds 5–7 are imidazopyridine fragment-like bearing 3,4-



Scheme 1. Synthetic routes and sets of modifications into the imidazopyridine/pyrimidine I (~21–92%), II (~54–86%) and Mannich-type scaffolds III (~38–97%). Reagents and conditions: a) appropriate bromoacetophenone, NaHCO₃, MeOH, reflux, 12 h; b) triphosgene, Et₃N, CH₂Cl₂, 0 °C and then appropriate 2° amine, 0 °C to 25 °C, 15 h or c) appropriate acyl chloride, Et₃N, CH₂Cl₂, 0 °C to 25 °C, 16 h; d) appropriate amine, formalin, acetic acid, CH₂Cl₂, 18 h.



Scheme 2. Synthetic routes and sets of modifications into the furopyridine scaffold (V: ~14–41%; VI: 18–67%; VII: 87%; VIII: 44%). Reagents and conditions: e) appropriated acyl chloride, DBU, DMAP, CH₂Cl₂, RT, overnight; f) mCPBA, CH₂Cl₂, RT, 48 h; g) appropriate 2° amine, PyBroP, DIPEA, MeCN, RT, 18 h; h) LiOH, THF/EtOH/H₂O, 55 °C, 24 h; i) MeNH₂·HCl, EDCI, HOBT, DMF, Et₃N, 25 °C, N₂, 4 h.

difluorophenyl (5 and 6) and phenyl groups (7) at the 2-position of the imidazole region of the backbone (R³). In addition, compound 6 has a (dimethylamino)methyl in region R² and compound 7 has a methyl group at the position R¹ and X. Analogs 8–14 are imidazopyrimidine amides retaining a phenyl substituent on the same imidazole portion mentioned before

and showing modifications in region R¹. Compound D and 15 have an electron withdrawing substituents on the imidazopyrimidine system (R³) with a 3-fluoropyrrolidinyl urea in region R¹. Compounds 16–19 have a 6-methyl-2-phenylimidazo[1,2-a]pyridine as the central core and diverse phenyl groups in region R³. Additionally, a set of 20 alkylamine-type compounds in the

side chain of the imidazo[1,2-*a*]pyridine core ring was synthesized. The synthetic route provided efficient ways to introduce substituents via the Mannich reaction at region R^2 (analogs 21–40). The hit compound **D** embedded with the 4-fluorophenylpiperazinyl group resulted in compound **56**. Compounds **20** and **57** are side products of the Mannich reaction, and we isolated and purified these compounds as well.

We took the opportunity to employ robust synthetic routes to further alter the internal portion of the imidazopyridine core and introduce different functional groups at different positions of the general scaffold, which led to the fused ring furopyridine derivatives 41–55 (Scheme 2). Recently our group reported a concise strategy to synthesize and decorate this core through C–H activation reaction.^[23] The synthesis of furo[2,3-*b*]pyridines started from pyridine-*N*-oxide derivative (**IV**).^[23] Under mild, metal-free conditions, we synthesized the furopyridines derivatives 41–44 with appropriated acyl chlorides (**V**). In addition, we functionalized this heteroaromatic core through C–H amination (**VI**, compounds 45–53). Carboxylic acid derivative **54** (**VII**) was obtained through ester hydrolysis. The following coupling reaction afforded the amide derivative **55** (**VII**). Analogs 41–45 are furopyridines bearing different phenyl groups in region R^3 of the backbone (2-position) and an ethyl ester group in the side chain in region R^2 of the furan moiety (3-position). Compounds 46–55 have a methyl or isopropyl group in region R^3 and *N*-cycloalkyl groups at different positions (R^1 , **V** or **X**).

Antitrypanosomal activities and cytotoxicity

Compounds 1–55 were tested in vitro against *T. cruzi*^[24] and *T. brucei* using EC_{50} and EC_{90} protocols.^[25] Assay results are presented in Table 1. Additionally, we retested the hit compound **D** and the new compounds **56** and **57** using IC_{50} protocols against *T. cruzi* and *T. brucei* (Table 1). Experimental details are provided in Supporting Information and in the literature.^[24–26]

Fast analysis of the antitrypanosomal activities reveals that 14 compounds are totally inactive against both parasites (EC_{50} values of *T. cruzi* and *T. brucei* > 20.0 μ M). Additional 17 compounds are also inactive against *T. brucei*, but some of them displayed high potencies against *T. cruzi*. Notably, this set of compounds exhibited better *T. cruzi* than *T. brucei* activities. Twenty-nine compounds showed anti-*T. cruzi* potency and 19 compounds showed anti-*T. brucei* potency lower than 10 μ M. It suggests that a more detailed analysis of the underlying structure–activity relationships would be of interest.

Furthermore, cytotoxicity was evaluated in mammalian cells (lymphocytic cells – CRL-8155 and hepatocellular cells – HepG2) and selectivity index (SI) calculated for selected compounds and compared to the published results for compound **D**^[13] (Table 2).

Only compounds **28** and **52** exhibited low toxicity to the CRL-8155 cell line, at 33.0 and 23.70 μ M, respectively. The remaining compounds exhibited no considerable or detectable toxicity to either cell line.

The selectivity ratio of compounds for *T. cruzi* and *T. brucei* parasites over each of the two cell lines was calculated. As an

example, the most active compound **15** exhibited a selectivity index (SI) > 625 for *T. cruzi* and > 1667 for *T. brucei* against either cell line, comparable to the hit compound **D**.

Compounds **D**, **56** and **57** were also screened against *T. b. rhodesiense*, *Leishmania infantum* and cytotoxicity for MCR-5 and PMM cells. Besides the already known biological activity of the compound **D** against *T. cruzi* and *T. brucei*,^[13] this compound also exhibited high biological activity against *T. b. rhodesiense* (IC_{50} of 0.11 μ M). Compounds **56** and **57** showed anti-*T. b. rhodesiense* activities of 0.90 μ M and 1.06 μ M, respectively. However, these three compounds were not potent against *L. infantum*. Marginal cytotoxicity was observed only for compound **D** against PMM cells (IC_{50} of 48.0 μ M) and no cytotoxicity against MRC-5 cell line.

Structure–activity relationships (SAR)

We discussed the SAR of heterocyclic compounds based on the wide range of biological activity obtained against *T. cruzi*^[24] and *T. brucei*^[25] for compounds **D** and 1–57. In order to accomplish this in a feasible way, we divided and discussed the substitutions systematically introduced into specific regions (R^1 – R^3) and positions (**V**–**Z**) of 3 distinct general scaffolds: imidazopyrimidine (15 analogs), imidazopyridine (28 analogs) and furopyridine (15 analogs). The following, we discuss the most representatives SARs established in this work.

The attempts to optimize the imidazopyrimidine scaffold is shown in Figure 2. The different regions of the molecule (R^1 – R^3) were explored with 14 variants. At the left of Figure 2 the SAR analysis for the region R^1 is presented. At the bottom and top right the SAR analysis for the region R^2 and variants for the region R^3 , respectively. Analogs 1–15 were assayed against *T. cruzi* (highlighted in green), *T. brucei* (highlighted in orange) and the results are expressed as EC_{50} (μ M).

Compounds **1** and **8**–**14** bear a phenyl group in region R^3 and hydrogen atom in region R^2 . Thus, the evaluation of the SAR was based on replacements in region R^1 . The addition of a phenyl carbamate group (**1** vs **8**) or even the introduction of a nitro group at *para*-position of the phenyl moiety (**8** vs **9**) had no effect in the potency against both parasites. However, moving the nitro group to *meta*-position enhanced the potency against *T. brucei* by more than 5-fold (**9** vs **10**). Compound **10** showed an EC_{50} value against *T. brucei* of 3.88 μ M. Replacing the oxygen atom in the phenyl carbamate group for a methylene linker (**8** vs **11**) resulted in low anti-*T. cruzi* activity (**11**, EC_{50} *T. cruzi* of 14.20 μ M). It appears that the cyclic aliphatic amide is better than an aromatic group in the region R^1 for achieving potency against *T. cruzi* (**8** vs **12**). Cyclohexylacetamide derivative **12** had an EC_{50} value against *T. cruzi* of 6.27 μ M.

T. cruzi activity was not affected by the exploration of the substitution pattern on the aromatic ring. Compounds **13** (R^1 = 4-cyanophenyl) and **14** (R^1 = 3,4-difluoro phenyl) showed an EC_{50} value against *T. cruzi* around 10.0 μ M, although the effect of the cyano group was more pronounced against *T. brucei* (EC_{50} *T. brucei* of 4.45 μ M) than against *T. cruzi* (EC_{50} *T. cruzi* of 10.33 μ M).

Table 1. Antitrypanosomal activities of heterocyclic compounds

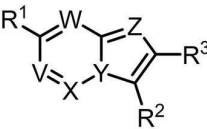
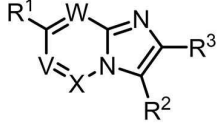
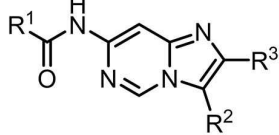
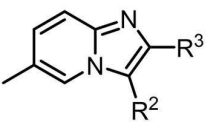
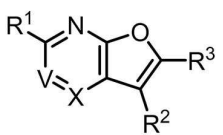
<div style="text-align: center;">  <p>General Scaffold</p> </div>								
<div style="display: flex; justify-content: space-around; align-items: flex-end;"> <div style="text-align: center;">  <p>1-7</p> </div> <div style="text-align: center;">  <p>D, 8-15, 56 and 57</p> </div> <div style="text-align: center;">  <p>16-40</p> </div> <div style="text-align: center;">  <p>41-55</p> </div> </div>								
Compd.	R ¹	R ²	R ³	V, W, X = CH unless otherwise noted	<i>T. cruzi</i> EC ₅₀ [μM]*	EC ₉₀ [μM]*	<i>T. brucei</i> EC ₅₀ [μM]**	EC ₉₀ [μM]**
1	NH ₂	H	phenyl	V = N	> 20.0	> 20.0	> 20.0	> 20.0
2	NH ₂	H	3,4-difluorophenyl	V = N	> 20.0	> 20.0	> 20.0	> 20.0
3	NH ₂	H	3-trifluoromethylphenyl	V = N	> 20.0	> 20.0	> 20.0	> 20.0
4	H	H	3,4-difluorophenyl	W = N	> 20.0	> 20.0	> 20.0	> 20.0
5	H	H	3,4-difluorophenyl	–	> 20.0	> 20.0	> 20.0	> 20.0
6	H	CH ₂ N(CH ₃) ₂	3,4-difluorophenyl	–	> 20.0	> 20.0	> 20.0	> 20.0
7	CH ₃	H	phenyl	X = CCH ₃	7.2	13.4	> 20.0	> 20.0
8	phenoxy	H	phenyl	–	> 20.0	> 20.0	> 20.0	> 20.0
9	4-nitrophenoxy	H	phenyl	–	> 20.0	> 20.0	> 20.0	> 20.0
10	3-nitrophenoxy	H	phenyl	–	9.8	> 20.0	3.9	10.9
11	benzyl	H	phenyl	–	14.2	> 20.0	> 20.0	> 20.0
12	cyclohexylmethyl	H	phenyl	–	6.3	7.3	12.3	> 20.0
13	4-cyanophenyl	H	phenyl	–	10.3	> 20.0	4.4	> 20.0
14	3,4-difluoro	H	phenyl	–	10.5	> 20.0	> 20.0	> 20.0
15	(3S)-3-fluoropyrrolidin-1-yl	H	3-trifluoromethylphenyl	–	0.08	0.09	0.03	0.05
16	–	H	phenyl	–	> 20.0	> 20.0	> 20.0	> 20.0
17	–	H	4-methylphenyl	–	> 5.0	> 5.0	5.9	> 20.0
18	–	H	4-chlorophenyl	–	> 5.0	> 5.0	10.4	> 20.0
19	–	H	3,4-difluorophenyl	–	> 5.0	> 5.0	12.3	> 20.0
20	–	CH ₂ OH	3,4-difluorophenyl	–	> 5.0	> 5.0	> 20.0	> 20.0
21	–	CH ₂ N(CH ₃) ₂	phenyl	–	> 20.0	> 20.0	> 20.0	> 20.0
22	–	3-(trifluoromethyl)phenylaminemethyl	phenyl	–	> 20.0	> 20.0	> 20.0	> 20.0
23	–	pyrrolidin-1-ylmethyl	phenyl	–	> 20.0	> 20.0	> 20.0	> 20.0
24	–	piperidin-1-ylmethyl	phenyl	–	15.0	> 20.0	> 20.0	> 20.0
25	–	morpholin-4-ylmethyl	phenyl	–	13.4	> 20.0	> 20.0	> 20.0
26	–	(3S)-3-fluoropyrrolidin-1-ylmethyl	phenyl	–	8.6	> 20.0	> 20.0	> 20.0
27	–	4-phenylpiperazin-1-ylmethyl	phenyl	–	5.2	9.7	9.9	10.1
28	–	4-(2,3-dichlorophenyl)piperazin-1-ylmethyl	phenyl	–	3.3	6.5	9.9	10.1
29	–	4-(4-chlorophenyl)piperazin-1-ylmethyl	phenyl	–	1.9	6.5	7.2	8.9
30	–	4-phenylpiperazin-1-ylmethyl	3,4-difluorophenyl	–	1.6	3.6	8.0	11.6
31	–	4-(4-fluorophenyl)piperazin-1-ylmethyl	3,4-difluorophenyl	–	1.0	3.6	6.2	11.8
32	–	4-[3-(trifluoromethyl)phenyl]piperazin-1-ylmethyl	3,4-difluorophenyl	–	1.6	4.1	3.3	4.6
33	–	4-(4-fluorophenyl)piperazin-1-ylmethyl	4-chlorophenyl	–	1.1	3.3	5.9	12.8
34	–	4-[3-(trifluoromethyl)phenyl]piperazin-1-ylmethyl	4-chlorophenyl	–	1.7	> 5.0	6.6	11.4
35	–	4-(4-fluorophenyl)piperazin-1-ylmethyl	4-methylphenyl	–	1.0	3.4	6.9	7.8
36	–	4-[3-(trifluoromethyl)phenyl]piperazin-1-ylmethyl	4-methylphenyl	–	1.5	> 5.0	5.2	> 20.0
37	–	4-cyclohexylpiperazin-1-ylmethyl	3,4-difluorophenyl	–	2.6	> 5.0	> 20.0	> 20.0
38	–	4-[2-(pyridin-3-yl)ethyl]piperazin-1-ylmethyl	3,4-difluorophenyl	–	1.8	> 5.0	> 20.0	> 20.0
39	–	4-benzylpiperidin-1-ylmethyl	3,4-difluorophenyl	–	1.6	4.7	16.6	18.1

Table 1. continued

<div style="text-align: center;"> <p>General Scaffold</p> </div>								
<div style="display: flex; justify-content: space-around; align-items: flex-end;"> <div style="text-align: center;"> <p>1-7</p> </div> <div style="text-align: center;"> <p>D, 8-15, 56 and 57</p> </div> <div style="text-align: center;"> <p>16-40</p> </div> <div style="text-align: center;"> <p>41-55</p> </div> </div>								
Compd.	R ¹	R ²	R ³	V, W, X = CH unless otherwise noted	<i>T. cruzi</i> EC ₅₀ [μM]*	EC ₉₀ [μM]*	<i>T. brucei</i> EC ₅₀ [μM]**	EC ₉₀ [μM]**
40	–	4-phenylpiperidin-1-ylmethyl	3,4-difluorophenyl	–	1.1	> 5.0	7.6	9.6
41	H	COOCH ₂ CH ₃	phenyl	–	14.7	> 20.0	> 20.0	> 20.0
42	H	COOCH ₂ CH ₃	4-fluorophenyl	–	13.8	> 20.0	18.9	> 20.0
43	H	COOCH ₂ CH ₃	3,4-difluorophenyl	–	10.9	> 20.0	10.3	> 20.0
44	H	COOCH ₂ CH ₃	4-methylphenyl	–	8.6	18.9	17.5	> 20.0
45	(3S)-3-fluoropyrrolidin-1-yl	COOCH ₂ CH ₃	4-methylphenyl	–	10.9	> 20.0	> 20.0	> 20.0
46	(3S)-3-fluoropyrrolidin-1-yl	COOCH ₂ CH ₃	CH ₃	–	17.3	> 20.0	> 20.0	> 20.0
47	H	COOCH ₂ CH ₃	CH ₃	V = C-(3S)-3-fluoropyrrolidin-1-yl	18.9	> 20.0	14.5	> 20.0
48	morpholin-4-yl	COOCH ₂ CH ₃	CH ₃	–	17.4	> 20.0	> 20.0	> 20.0
49	morpholin-4-yl	COOCH ₂ CH ₃	C(CH ₃) ₂	–	4.8	18.4	> 20.0	> 20.0
50	4-phenylpiperazin-1-yl	COOCH ₂ CH ₃	CH ₃	–	3.4	6.4	> 20.0	> 20.0
51	4-phenylpiperazin-1-yl	COOCH ₂ CH ₃	C(CH ₃) ₂	–	11.0	> 20.0	> 20.0	> 20.0
52	H	COOCH ₂ CH ₃	C(CH ₃) ₂	X = C-4-phenylpiperazin-1-yl	7.1	9.2	9.8	13.8
53	pyrrolidin-1-yl	COOCH ₂ CH ₃	C(CH ₃) ₂	–	4.5	> 20.0	> 20.0	> 20.0
54	pyrrolidin-1-yl	COOH	C(CH ₃) ₂	–	> 20.0	> 20.0	> 20.0	> 20.0
55	pyrrolidin-1-yl	CONHCH ₃	C(CH ₃) ₂	–	> 20.0	> 20.0	> 20.0	> 20.0
***56	(3S)-3-fluoropyrrolidin-1-yl	4-(4-fluorophenyl)piperazin-1-ylmethyl	3,4-difluorophenyl	–	10.42	–	0.95	–
***57	(3S)-3-fluoropyrrolidin-1-yl	CH ₂ OH	3,4-difluorophenyl	–	18.97	–	1.21	–
***D	(3S)-3-fluoropyrrolidin-1-yl	H	3,4-difluorophenyl	–	0.73	–	0.21	–

Compounds 1–55: * the values are averages of triplicate data. Benznidazole was used as a control compound for the *T. cruzi* assay, with EC₅₀ and EC₉₀ values (average ± SEM) 0.65 ± 0.10 μM (n = 5) and 1.64 ± 0.09 μM (n = 5). ** Pentamidine was used as a control compound for the *T. brucei* assays, with EC₅₀ and EC₉₀ values (average ± SEM) of 1.24 ± 0.23 nM (n = 5) and 6.20 ± 2.12 nM (n = 5). **Compounds 56, 57 and D:** ***activity is expressed as IC₅₀ values in μM concentrations. The values of *T. cruzi* and *T. brucei* activities are averages of duplicate data (average ± SD). Benznidazole (IC₅₀ of 2.43 ± 0.45 μM) and Suramine (IC₅₀ of 0.06 ± 0.01 μM) were used as reference drugs to measure *T. cruzi* and *T. brucei* activities, respectively.

Compounds **3** and **15** are analogs bearing 3-trifluoromethylphenyl substituent in region R³ and hydrogen atom in region R². Substantial enhancement of activity was achieved by the introduction of a 3-fluoropyrrolidinyl urea group in region R¹ of the imidazopyrimidine system. This substitution enhanced the potency of compound **15** more than 250-fold against *T. cruzi* and more than 660-fold against *T. brucei*, when compared to compound **3** (R¹ = NH₂). Compound **15** exhibited an EC₅₀ value against *T. cruzi* of 0.08 μM and against *T. brucei* of 0.03 μM (Figure 2).

The same pattern can be observed for the amide derivatives compared to the urea derivatives **D** and **15**, the presence of the

urea group attached to the region R¹ of the fused ring system proved to be essential for bioactivity. Compounds **D** and **15** are nanomolar inhibitors of *T. cruzi* and *T. brucei*, while some of the amide derivatives showed moderate activity only against one of these parasites.

According to the literature compounds bearing methyl-*N,N*-substituted amines (phenylpiperazines) could be an attractive group to increment potency for anti-infective agents against trypanosomiasis.^[27–29] We then used the strategy of combining chemical substructures found in the literature, with the highly active compound **D** to derive new compounds, but keeping the skeleton unaltered. Embedding the 4-

Table 2. Cytotoxicity and Selectivity index (SI) for Selected Compounds

Compd	<i>T. cruzi</i> EC ₅₀ [μM]	<i>T. brucei</i> EC ₅₀ [μM]	Hep G2 ^[a,b] EC ₅₀ [μM]	SI ^[e] <i>T. cruzi</i>	<i>T. brucei</i>	CLR-8155 ^[c,d] EC ₅₀ [μM]	SI ^[e] <i>T. cruzi</i>	<i>T. brucei</i>
***D	0.09	0.02	> 50.0	556	2500	> 50.0	556	2500
15	0.08	0.03	> 50.0	625	1667	> 50.0	625	1667
17	> 5.0	5.9	> 50.0	10	8	41.3	8	7
22	> 20.0	> 20.0	> 50.0	3	3	> 50.0	3	3
23	> 20.0	> 20.0	> 50.0	3	3	> 50.0	3	3
24	15.0	> 20.0	> 50.0	3	3	> 50.0	3	3
25	13.4	> 20.0	> 50.0	4	3	> 50.0	4	3
26	8.6	> 20.0	> 50.0	6	3	> 50.0	6	3
27	5.2	9.9	> 50.0	10	5	> 50.0	10	5
28	3.3	9.9	> 50.0	15	5	33.0	10	3
29	1.9	7.2	> 50.0	26	7	49.0	26	7
30	1.6	8.0	> 50.0	31	6	> 50.0	31	6
31	1.0	6.2	> 50.0	49	8	42.9	42	7
32	1.6	3.3	> 50.0	30	15	> 50.0	30	15
33	1.1	5.9	> 50.0	43	8	> 50.0	43	8
34	1.7	6.6	> 50.0	29	8	> 50.0	29	8
35	1.0	6.9	–	–	–	> 50.0	50	7
36	1.50	5.2	–	–	–	47.6	32	9
38	1.8	> 20.0	40.6	23	2	> 50.0	28	3
39	1.6	16.6	> 50.0	30	3	> 50.0	30	3
40	1.1	7.6	> 50.0	45	7	> 50.0	45	7
44	8.6	17.5	> 50.0	6	3	> 50.0	6	3
45	10.9	> 20.0	> 50.0	5	3	> 50.0	5	3
49	4.8	> 20.0	> 50.0	10	3	> 50.0	10	3
50	3.4	> 20.0	> 50.0	15	3	> 50.0	15	3
52	7.1	9.8	> 50.0	7	5	23.7	3	2
53	4.5	> 20.0	> 50.0	11	3	> 50.0	11	3

[a] Human hepatocytes (HepG2). Compounds were tested in quadruplicate. [b] Quinacrine was included as a control compound, with EC₅₀ and EC₉₀ values (average ± SEM) of 14.34 ± 4.51 μM (n = 3) and 18.74 ± 7.05 μM (n = 3). [c] Human lymphoblasts (CRL-8155). Compounds were tested in quadruplicate. [d] Quinacrine was included as a control compound, with EC₅₀ and EC₉₀ values (average ± SEM) of 5.47 ± 1.97 μM (n = 3) and 15.74 ± 4.54 μM (n = 3). [e] Selectivity index expressed as the ratio EC₅₀ (cell line)/EC₅₀ (*T. cruzi* or *T. brucei*), rounded to the nearest integer. ***reference [13].

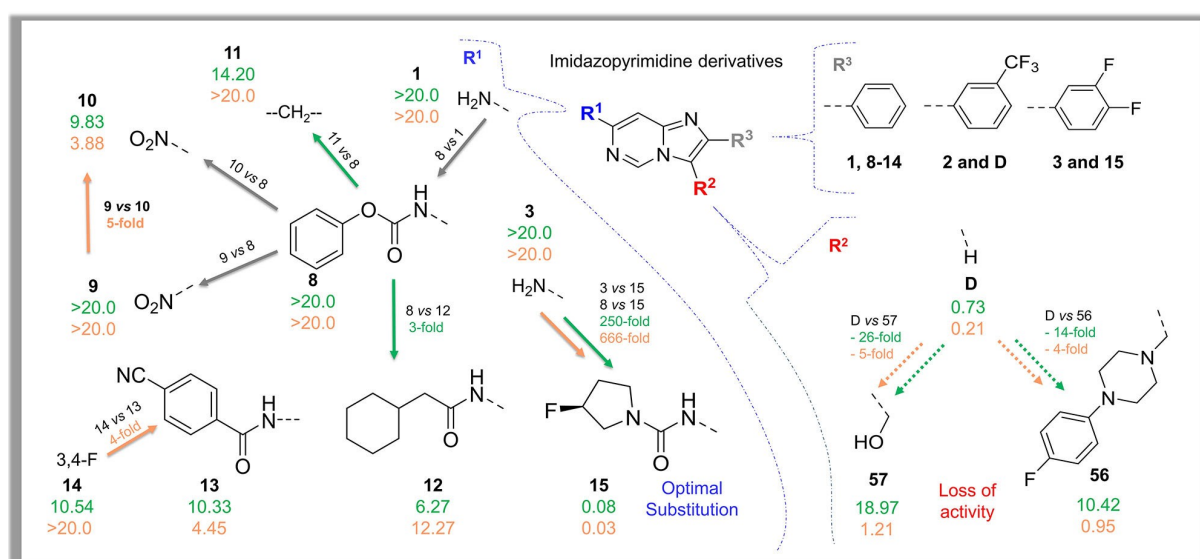


Figure 2. Modifications and EC₅₀ μM of the imidazopyrimidine core ring. Compounds assayed against *T. cruzi* (highlighted in green)/*T. brucei* (highlighted in orange). All the results are expressed as EC₅₀ (μM); except for compounds D, 56 and 57 IC₅₀ (μM). Green and orange arrows represent the improvement of the *T. cruzi* and *T. brucei* activities, respectively. Green and orange dashed arrows represent the loss of the *T. cruzi* and *T. brucei* activities, respectively. Gray arrow represents no improvement of the antitrypanosomal activities.

fluorophenylpiperazinylmethyl (R^2) into the compound D with the combination of 3-fluoropyrrolidinyl urea group in region R^1 and 3,4-difluorophenyl group in region R^3 did not improve the

antitrypanosomal activities (D vs 56). The activity of compound 56 decreased more than 4-fold against both parasites.

The incorporation of the hydroxymethyl functional group ($-\text{CH}_2\text{OH}$) in region R^2 (57) resulted in similar antitrypanosomal activities as compound 56. However, hydroxymethyl group can be a versatile point of diversification to access other target compounds; to alter physicochemical properties such as lipophilicity ($\log\text{-P}$), solubility and through hydrogen-bonding interactions, the mode of binding of the pharmacophore.^[30] In these two compounds the combination of the best moiety present in region R^1 and R^3 of analog D, plus the alteration of the imidazo portion has not shown to be synergistic, *i.e.* compounds 56 and 57 risen from this approach have shown bioactivities lower than D. Aiming to explore and evaluate the SAR for modifications only in region R^2 , a neutral scaffold was chosen. That means an absence of substituents in region R^1 and an exchange of a basic nitrogen atom for a methyl group at the 6-position of the imidazopyrimidine core (Figure 2); which turned into a new scaffold 6-methylimidazo[1,2-*a*]pyridine (Figure 3).

The introduction of dimethylmethanamine (21), 3-(trifluoromethyl)phenylaminemethyl (22) and pyrrolidinylmethyl (23) as substituents in region R^2 , resulted in inactive compounds (Figure 3). Replacements with piperidinylmethyl (24, EC_{50} of 15.04 μM), morpholinylmethyl (25, EC_{50} of 13.40 μM) and (3S)-3-fluoropyrrolidinylmethyl groups (26, EC_{50} of 8.61 μM) showed only low potency against *T. cruzi* (Figure 3, highlighted in green).

However, the insertion of a phenylpiperazinylmethyl moiety in region R^2 of the imidazole portion (Figure 3, bottom right) showed to be promising to enhance antitrypanosomal activity (16 vs 28 and 29). The introduction of chloride atoms at the phenyl group attached at the piperazine at the 4- and 2,3-positions enhanced only *Anti-T. cruzi* potency. Phenylpiperazines derivatives 28 and 29 exhibited EC_{50} values of 3.31 and 1.90 μM , respectively. In fact, upon embedding phenylpiperazinylmethyl in region R^2 of the imidazole portion an enhancement in potency for the *T. brucei* compared to *T. cruzi* potencies was not observed. While some compounds showed EC_{50} about 1.0 μM against *T. cruzi*, most of the compounds showed EC_{50} above to 5.0 μM against *T. brucei*.

Bulky aminoalkyl groups in the side chain of imidazopyridine derivatives are clearly required for better anti-*T. cruzi* activity. About 11 compounds bearing bulky aminoalkyl groups achieved potency lower than 2 μM only against *T. cruzi*.

Moreover, inserting electron-withdrawing groups (31 and 32) or exchanging the aromatic portion of the piperazine (37–39) did not modify the potency against *T. cruzi* (Figure 3, bottom left). At the same time, the activities of compounds 37–39 reveal that the presence of more flexible groups in region R^2 did not contribute to enhancing the potency against *T. brucei*. The compounds display above 7 times better *T. cruzi* potency than *T. brucei* potency.

Furthermore, the SAR were explored diversifying phenyl groups in region R^3 of the imidazole portion. The methylation

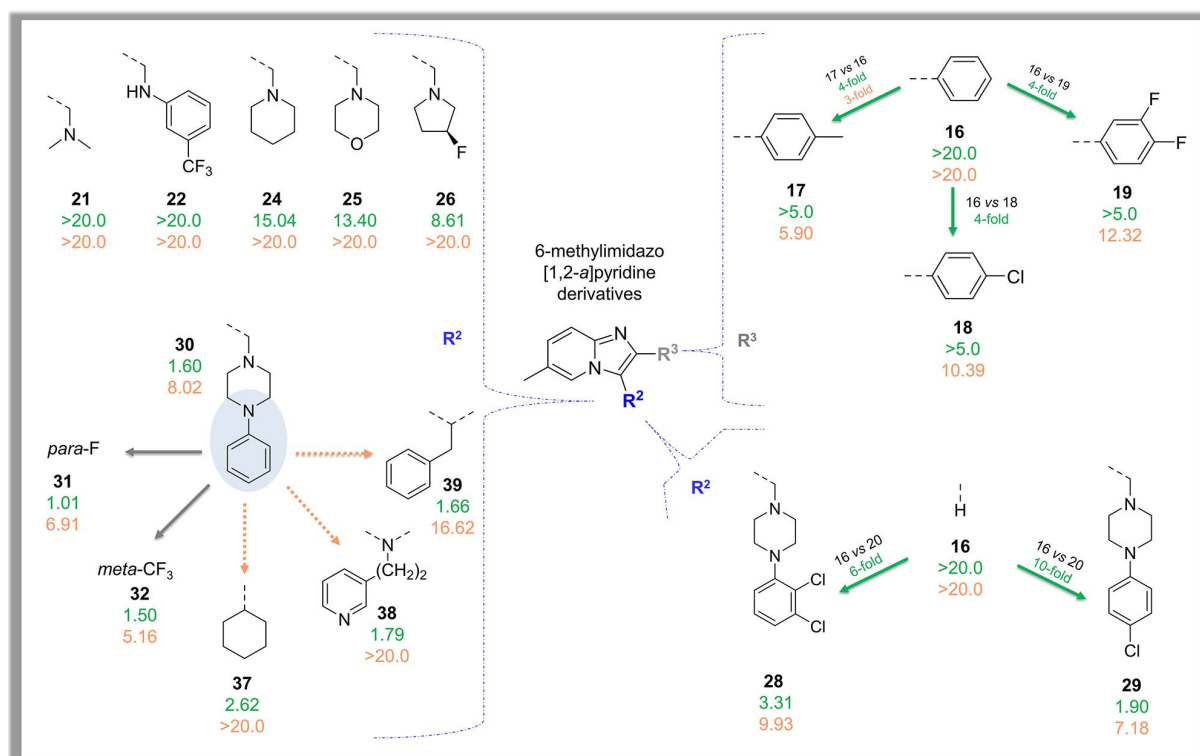


Figure 3. Modifications of the 6-methyl-2-phenylimidazo[1,2-*a*]pyridine core ring. Compounds assayed against *T. cruzi* (highlighted in green)/*T. brucei* (highlighted in orange). Results are expressed as EC_{50} (μM). Green arrows represent the improvement of the *T. cruzi* activity. Orange dashed arrows represent the loss of the *T. brucei* activity. Gray arrows represent no improvement of the antitrypanosomal activities

(17), chlorination (18) or difluorination (19) conferred a slight improvement in potencies compared to **16** (Figure 3, top right). A similar pattern was observed for the pairs of compounds containing replacements of the aromatic ring attached in region R^3 (pairs: **31** vs **33**; **32** vs **34**; **31** vs **35**; **32** vs **36**, Table 1).

Subsequently, altering the core ring system from an imidazopyridine/pyrimidine to a furo[2,3-*b*]pyridine allowed us to expand the chemical space of new heterocyclic compounds as potential antitrypanosomal agents. We selected substituents from our previous SAR and we also introduced new modifications into the core ring of furopyridines, such as aliphatic groups in region R^3 or functional groups in region R^2 . Figure 4 shown the selected SAR analysis for each region.

Fluorination or methylation (**41** vs **42–44**) of the aromatic ring attached to the 2-position of furopyridine (R^3) had no impact on the potency of this class of compounds. Despite that, isopropyl and methyl groups appeared to be more promising than aromatic groups in this region. Compound **49** and **50** exhibited EC_{50} values of 4.81 and 3.40, respectively (Figure 4, top right). We also verified that the ester group in region R^2 was necessary for the activity of this class against *T. cruzi* (**53** vs **54**, **55**). We further evaluated the amine fragments, such as morpholine, phenylpiperazine and (3*S*)-3-fluoropyrrolidinyl, in the activity of our furopyridine framework (**46** and **48** vs **50**). Repeatedly in this SAR studies, the phenylpiperazine moiety has appeared to be promising to achieve gains in potency against *T. cruzi* (Figure 4, top left). Compound **50** (EC_{50} of 3.40 μ M) is 5-fold more potent than the derivatives containing (3*S*)-3-fluoropyrrolidinyl (**46**, EC_{50} of 17.29 μ M) and morpholinyl groups (**48**, EC_{50} of 17.36 μ M). The relocation of the (3*S*)-3-fluoropyrrolidinyl or phenylpiperazine moiety did not result in any benefits to antitrypanosomal activities (**47** and **52**). Meanwhile, the phenylpiperazine attached at the X-position was the unique replacement that resulted in *T. brucei* activity below 10 μ M.

The fragment (3*S*)-3-fluoropyrrolidinyl which showed to be an important feature in the imidazopyrimidine framework of this series of compounds, did not display the same positive influence in the activity of some furopyridines (**45** and **47**), no matter the position placed. Probably, the absence of the functional urea group in this furopyridine class of compounds could be an explanation for no enhancement in the potency. In other words, the imidazopyrimidine series of compounds required a functional group containing a carbonyl group bonded to two nitrogen atoms. For example, compounds **D** and **15** achieved nanomolar potency against both parasites. In summary, our findings in the SAR analysis can guide further studies with this class of compounds.

Conclusion

The imidazopyridines/pyrimidines and furopyridines planned and obtained herein allowed us to build a SAR study by means of cell assays against *T. cruzi*, *T. brucei*, and mammalian cells. By exploring the chemical diversity of three different heteroaromatic cores and introducing various groups at eight different positions of the general scaffold within this study, we were able to enlarge the chemical space of heterocycles as potential antitrypanosomal agents. The central core was embedded with urea, amide, ester, and organic acid functions. However, the presence of the urea group attached to the 7-position (R^1) of the fused ring system proved to be essential for bioactivity (**D** and **15** are nanomolar inhibitors of *T. cruzi* and *T. brucei*). We introduced the furopyridine derivatives as a new core ring to be developed for antitrypanosomal agents. We explored aromatic and aliphatic replacements and employed different organic functions at the 3-position of the furan ring portion, respectively. In addition, we embedded four different groups at three

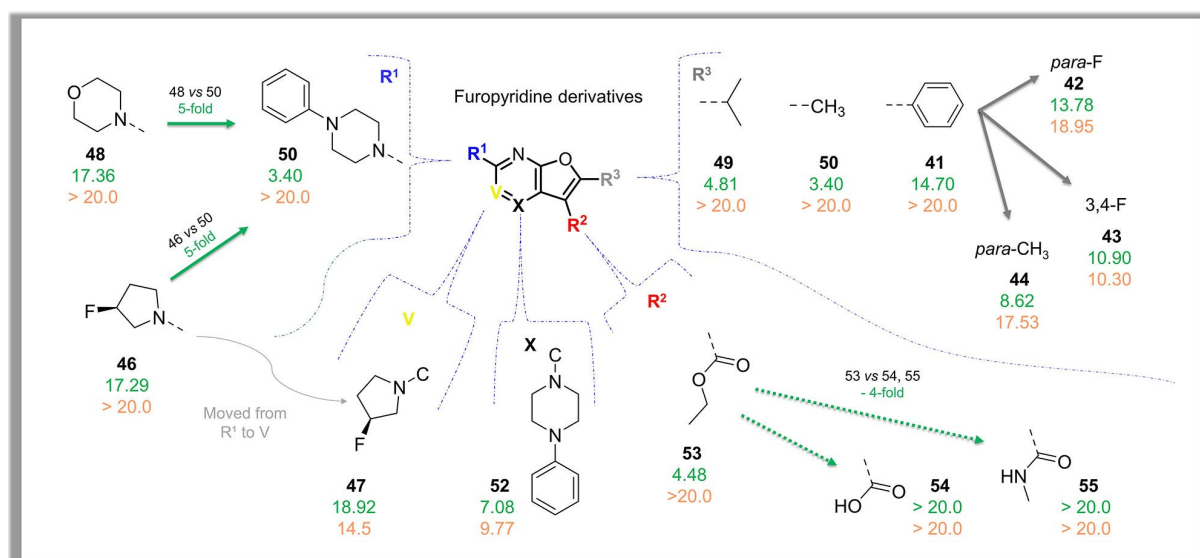


Figure 4. Modifications of the furo[2,3-*b*]pyridine core ring. Compounds assayed against *T. cruzi* (highlighted in green)/*T. brucei* (highlighted in orange). Results are expressed as EC_{50} (μ M). Green solid or dashed arrows represent the improvement or the loss of the *T. cruzi* activities, respectively. Gray arrow represents no improvement of the antitrypanosomal activities.

positions of the pyridine portion. However, we still need to combine promising substituents found through SAR in order to improve the potency of furopyridines as antitrypanosomal agents. The best replacements identified in this SAR studies, will guide the design and selection of the novel compounds that can be transitioned further into drug development for these parasitic infections.

Author contributions

The manuscript was written through the contributions of all authors. All authors have given approval to the final version of the manuscript. D.G.S. planned and synthesized 47 compounds. S.M.G.M. and F.F. planned and synthesized 10 compounds. Biological assays were performed by J.R.B., N.M., and A.M.

Acknowledgements

We are grateful to Fundação de Amparo à Pesquisa do Estado de São Paulo (FAPESP), Coordenação de Aperfeiçoamento de Pessoal de Nível Superior – Brasil (CAPES) – Finance Code 001 and Conselho Nacional de Desenvolvimento Científico e Tecnológico (CNPq) for funding [grant numbers: #88881.170193/2018-01 (D.G.S.), #2017/22001-0 (D.G.S.), #2017/21146-4 (F.S.E.), #313834/2018-0 (F.S.E.), #428527/2016-7 (F.S.E.)]. We thank Prof. Dr. Bernhard Wünsch for hosting Dr. Silva in his laboratory at the University of Münster (WWU) in Germany and also for helpful discussions to develop this work. Open access funding enabled and organized by Projekt DEAL.

Conflict of Interest

The authors declare no conflict of interest.

Keywords: Anti-infectives · heterocyclic · *T. brucei* · *T. cruzi* · in vitro

- [1] DNDi América Latina. 2020. [online] Available at: <https://www.dndi-l.org/> [Accessed 13 August 2020].
- [2] F. Olmo, C. Rotger, I. Ramírez-Macías, L. Martínez, C. Marín, L. Carreras, K. Urbanová, M. Vega, G. Chaves-Lemaire, A. Sampedro, M. J. Rosales, M. Sánchez-Moreno, A. Costa, *J. Med. Chem.* **2014**, *57*, 987–999.
- [3] J. J. Nogueira Silva, W. R. Pavanelli, F. R. Salazar Gutierrez, F. C. Alves Lima, A. B. Ferreira da Silva, J. Santana Silva, D. Wagner Franco, *J. Med. Chem.* **2008**, *51*, 4104–4114.
- [4] S. Garcia, C. O. Ramos, J. F. V. Senra, F. Vilas-Boas, M. M. Rodrigues, A. C. Campos-de-Carvalho, R. Ribeiro-dos-Santos, M. B. P. Soares, *Antimicrob. Agents Chemother.* **2005**, *49*, 1521–1528.
- [5] S. Russell, R. Rahmani, A. J. Jones, H. L. Newson, K. Neilde, I. Cotillo, M. Rahmani Khajouei, L. Ferrins, S. Qureshi, N. Nguyen, M. S. Martinez-

- Martinez, D. F. Weaver, M. Kaiser, J. Riley, J. Thomas, M. De Rycker, K. D. Read, G. R. Flematti, E. Ryan, S. Tanghe, A. Rodriguez, S. A. Charman, A. Kessler, V. M. Avery, J. B. Baell, M. J. Piggott, *J. Med. Chem.* **2016**, *59*, 9686–9720.
- [6] J. A. Urbina, R. Docampo, *Trends Parasitol.* **2003**, *19*, 495–501.
- [7] J. A. Castro, M. M. de Mecca, L. C. Bartel, *Hum. Exp. Toxicol.* **2006**, *25*, 471–479.
- [8] R. J. Pierce, J. MacDougall, R. Leurs, M. P. Costi, *Trends Parasitol.* **2017**, *33*, 581–583.
- [9] B. Zulfiqar, T. B. Shelper, V. M. Avery, *Drug Discovery Today* **2017**, *22*, 1516–1531.
- [10] H. B. Tatipaka, J. R. Gillespie, A. K. Chatterjee, N. R. Norcross, M. A. Hulverson, R. M. Ranade, P. Nagendar, S. A. Creason, J. McQueen, N. A. Duster, *J. Med. Chem.* **2014**, *57*, 828–835.
- [11] D. A. Patrick, T. Wenzler, S. Yang, P. T. Weiser, M. Z. Wang, R. Brun, R. R. Tidwell, *Bioorg. Med. Chem.* **2016**, *24*, 2451–2465.
- [12] D. A. Patrick, J. R. Gillespie, J. McQueen, M. A. Hulverson, R. M. Ranade, S. A. Creason, Z. M. Herbst, M. H. Gelb, F. S. Buckner, R. R. Tidwell, *J. Med. Chem.* **2017**, *60*, 957–971.
- [13] D. G. Silva, J. R. Gillespie, R. M. Ranade, Z. M. Herbst, U. T. T. Nguyen, F. S. Buckner, C. A. Montanari, M. H. Gelb, *ACS Med. Chem. Lett.* **2017**, *8*, 766–770.
- [14] R. R. Tidwell, D. A. Patrick, F. S. Buckner, M. H. Gelb, J. R. Gillespie, D. G. Silva, US10399966B2, **2017**.
- [15] S. Linz, J. Müller, H. Hübner, P. Gmeiner, R. Troschütz, *Bioorg. Med. Chem.* **2009**, *17*, 4448–4458.
- [16] B. Lemmer, *Physiol. Behav.* **2007**, *90*, 285–293.
- [17] A. Heidari, *J. Data Min. Genomics Proteomics* **2016**, *7*, e125.
- [18] S. Sirakanyan, A. Hovakimyan, A. S. Noravanyan, *Russ. Chem. Rev.* **2015**, *84*, 441.
- [19] M. T. Bilodeau, A. E. Balitza, J. M. Hoffman, P. J. Manley, S. F. Barnett, D. Defeo-Jones, K. Haskell, R. E. Jones, K. Leander, R. G. Robinson, A. M. Smith, H. E. Huber, G. D. Hartman, *Bioorg. Med. Chem. Lett.* **2008**, *18*, 3178–3182.
- [20] J. S. Debenham, C. B. Madsen-Duggan, R. B. Toupence, T. F. Walsh, J. Wang, X. Tong, S. Kumar, J. Lao, T. M. Fong, J. C. Xiao, C. R. C. Huang, C.-P. Shen, Y. Feng, D. J. Marsh, D. S. Stribling, L. P. Shearman, A. M. Strack, M. T. Goulet, *Bioorg. Med. Chem. Lett.* **2010**, *20*, 1448–1452.
- [21] A. Arcadi, S. Cacchi, S. Di Giuseppe, G. Fabrizi, F. Marinelli, *Org. Lett.* **2002**, *4*, 2409–2412.
- [22] F. Fumagalli, S. M. G. de Melo, C. M. Ribeiro, M. C. Solcia, F. R. Pavan, F. da Silva Emery, *Bioorg. Med. Chem. Lett.* **2019**, *29*, 974–977.
- [23] F. Fumagalli, F. da Silva Emery, *J. Org. Chem.* **2016**, *81*, 10339–10347.
- [24] F. S. Buckner, C. L. Verlinde, A. C. La Flamme, W. C. Van Voorhis, *Antimicrob. Agents Chemother.* **1996**, *40*, 2592–2597.
- [25] S. Shibata, J. R. Gillespie, A. M. Kelley, A. J. Napuli, Z. Zhang, K. V. Kovzun, R. M. Pefley, J. Lam, F. H. Zucker, W. C. Van Voorhis, E. A. Merritt, W. G. Hol, C. L. Verlinde, E. Fan, F. S. Buckner, *Antimicrob. Agents Chemother.* **2011**, *55*, 1982–1989.
- [26] S. Shibata, J. R. Gillespie, R. M. Ranade, C. Y. Koh, J. E. Kim, J. U. Laydbak, F. H. Zucker, W. G. Hol, C. L. Verlinde, F. S. Buckner, E. Fan, *J. Med. Chem.* **2012**, *55*, 6342–6351.
- [27] R. Paucar, R. Martín-Escobano, E. Moreno-Viguri, A. Azqueta, N. Cirauqui, C. Marín, M. Sánchez-Moreno, S. Pérez-Silanes, *Bioorg. Med. Chem.* **2019**, *27*, 3902–3917.
- [28] I. N. Wenzel, P. E. Wong, L. Maes, T. J. J. Müller, R. L. Krauth-Siegel, M. P. Barrett, E. Davioud-Charvet, *ChemMedChem* **2009**, *4*, 339–351.
- [29] G. Roman, *European J. Med. Chem.* **2015**, *89*, 743–816.
- [30] D. C. Blakemore, L. Castro, I. Churcher, D. C. Rees, A. W. Thomas, D. M. Wilson, A. Wood, *Nat. Chem.* **2018**, *10*, 383–394.

Manuscript received: August 13, 2020

Revised manuscript received: October 13, 2020

Accepted manuscript online: October 19, 2020

Version of record online: November 11, 2020